

AN APPLICATION OF REE-IN-TWO-PYROXENE THERMOMETRY TO LL CHONDRITES: EVIDENCE FOR MULTISTAGE METAMORPHISM AND A RUBBLE PILE PARENT BODY. N. Dygert¹, A.D. Patchen¹, N.R. Miller² and H.Y. McSween¹, ¹Department of Earth and Planetary Sciences, University of Tennessee, Knoxville (ndygert1@utk.edu), ²Department of Geological Sciences, University of Texas at Austin.

Introduction: Models of the thermal evolution of meteorite parent asteroids are predicated on geothermometric estimates of temperatures and cooling rates achieved on those bodies [e.g., 1]. However, geothermometers used to constrain the thermal evolution of asteroids typically record blocking temperatures during cooling rather than peak or magmatic temperatures. Recently, a REE-in-two pyroxene thermometer was developed [2] which relies on the relatively slow diffusive exchange of REEs between coexisting pyroxenes, and has been shown to record near-peak or magmatic temperatures for samples from a variety of geologic settings in Earth's mantle and crust, and some samples from planetary environments [2-5]. Here, we apply the REE-in-two pyroxene thermometer to four LL ordinary chondrites to gain new insights into their thermal history, and to evaluate the geologic evolution of their parent body.

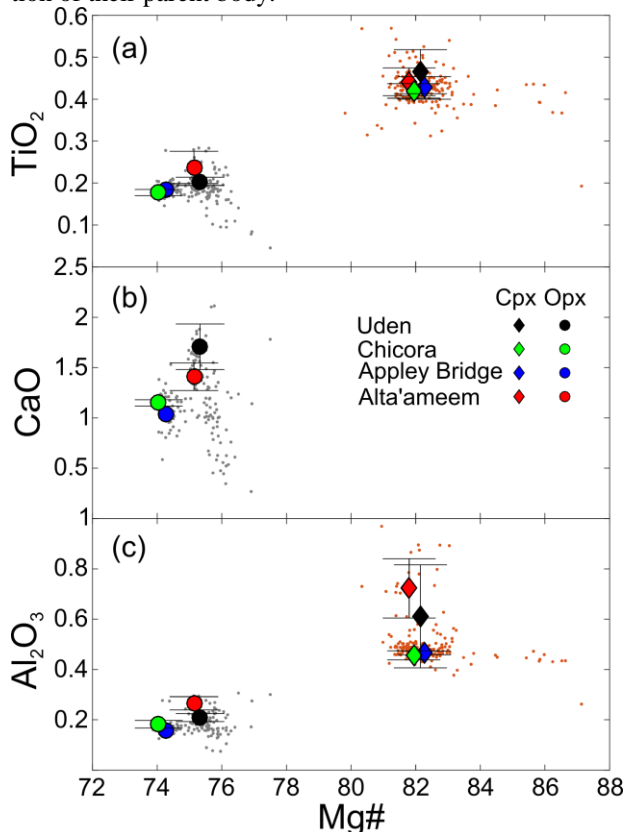


Figure 1. Major element variations. Small gray and orange dots (opx and cpx, respectively) show the range of compositions among all samples; large circles and diamonds are averaged compositions of grains analyzed by LA-ICP-MS.

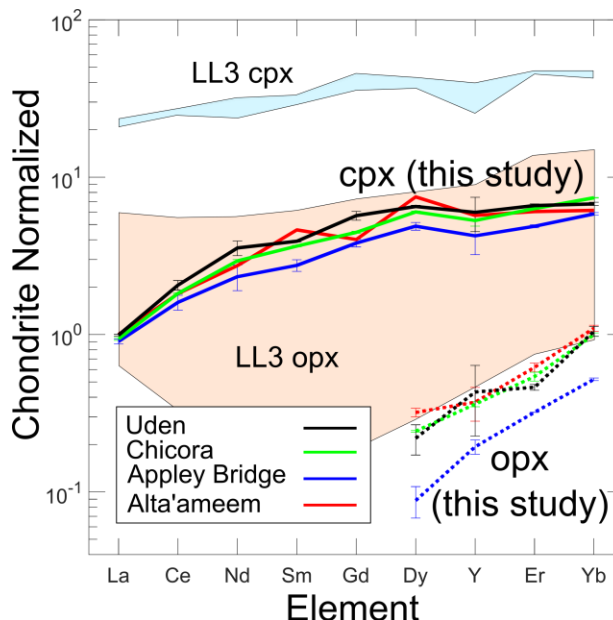


Figure 2. Chondrite normalized REE+Y abundances in cpx (solid lines) and opx (dotted lines). Error bars are 1σ standard deviations of replicate analyses. Shown for comparison are the range of values in three LL3 chondrites [7] (cyan and pink fields).

Samples and Methods: We selected Uden, Chicora, Appley Bridge, and Alta'ameem for analysis because of their high but variable metamorphic grades (7, 6, 6 and 5, respectively), and because their major element compositions and two-pyroxene temperatures were characterized by [6], providing a useful benchmark for comparison. Standard thickness thin sections were provided by the NMNH. Clinopyroxene (cpx) and orthopyroxene (opx) were identified using X-ray maps and analyzed by WDS spectrometry at the University of Tennessee with a focused 15nA, 30kV beam. Selected REEs, Y, Ti, Zr and Sc were measured in cpx and opx by LA-ICP-MS at the University of Texas at Austin at a laser fluence of 1.75 J/cm² at 8 Hz. We focused our attention on the largest inclusion-free grains we could identify, particularly those in close proximity to one another to maximize the potential for chemical equilibrium. This limited our laser spot sizes to 40-65 μ m; detection limits for REEs at the analytical conditions are ~20-60 ppb (depending on spot size).

Major and Trace Elements: Major elements are plotted in Fig. 1. Averaged compositions of grains analyzed by LA-ICP-MS are plotted using large symbols. Error bars show 1σ standard deviations and demonstrate compositional homogeneity suggesting a close approach to chem-

ical equilibrium. Chondrite normalized REE+Y abundances are shown in Fig. 2. Light-middle REEs in opx are below detection limits but Dy, Y, Er and Yb are sufficiently abundant for accurate characterization. Replicate analyses show good reproducibility. In Alta'ameem (LL5), trace element heterogeneity among opx in distinct clasts was observed; here we report opx and cpx data from a single clast. Although data are limited, in the other samples, trace elements appear to be homogeneous among clasts. In all samples, light-heavy REEs in cpx are above detection limits and replicate analyses show good reproducibility.

In comparison with LL3 chondrites [7], cpx and opx in the LL7-LL5 ordinary chondrites show less trace element variability among samples and less variability within individual samples (Fig. 2). The LL5-LL7 cpx and opx also have lower REE concentrations than the LL3s, presumably owing to sequestration of REEs by sulfides and phosphates during thermal metamorphism.

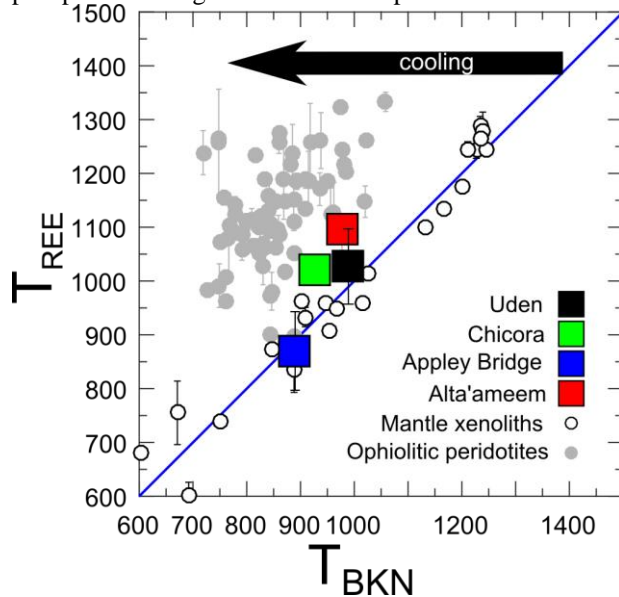


Figure 3. T_{REE} (y axis) plotted against T_{BKN} (x axis) ($^{\circ}\text{C}$). Ordinary chondrites are large squares; also shown are quenched mantle xenoliths from thermally stable environments [2,9] and ophiolitic peridotites that cooled slowly [3], which fall far to the left of the blue 1:1 line.

Temperatures: REE-in-two pyroxene temperatures (T_{REE}) are reported in Fig. 3 and the Table. T_{REE} (870–1097 $^{\circ}\text{C}$) are similar to or slightly higher than temperatures from the two pyroxene major element thermometer of Brey and Köhler (T_{BKN}) [8] (890–989 $^{\circ}\text{C}$). T_{REE} uncertainties are obtained from scatter in the multi-element temperature inversion; sources of uncertainty may include failure to attain thermodynamic equilibrium during metamorphism, or data quality issues. We view the Alta'ameem temperatures as the least reliable owing to the

sample's low metamorphic grade and the compositional heterogeneity we observed [c.f. 6].

Sample	Grade	T_{REE}	T_{BKN}	ΔT
Uden	LL7	1027 \pm 70	989	38
Chicora	LL6	1022 \pm 17	927	95
Appley Bridge	LL6	870 \pm 13	890	-20
Alta'ameem	LL5	1097 \pm 8	977	120

Inferences: At a temperature of 1000 $^{\circ}\text{C}$, REE lattice diffusion in opx is $\sim 10^{-22}$ m^2/s [10], such that characteristic diffusion timescales for grain sizes relevant to the ordinary chondrites (~ 100 μm) are ~ 1 Myr. Thus, we infer that these T_{REE} are peak or near peak temperatures. In contrast, T_{BKN} (which is based on relatively rapid temperature sensitive diffusive exchange of the diopside component between pyroxenes) often represent subsolidus cooling temperatures rather than peak temperatures. The difference between T_{REE} and T_{BKN} (ΔT) can be used to infer the cooling rate of a sample. Samples quenched from stable, high temperature environments (e.g., subcontinental mantle xenoliths, Fig. 3) have similar T_{REE} and T_{BKN} . Samples that cooled slowly (e.g., ophiolitic peridotites, Fig. 3) have higher T_{REE} than T_{BKN} . The agreement of T_{REE} and T_{BKN} among the LL chondrites implies these samples were rapidly cooled (quenched) from peak temperatures at $>900^{\circ}\text{C}$.

Simple closure temperature models suggest the meteorites cooled through T_{BKN} and T_{REE} blocking temperatures at rates $\geq 1^{\circ}\text{C}/\text{year}$ [11]. Such fast cooling is inconsistent with much slower rates inferred from metallography, Pb isotopes, fission tracks, and Ar-Ar dating, which are $\sim 1\text{--}40^{\circ}/\text{Myr}$ [12–15]. These techniques record cooling rates at temperatures $\leq 500^{\circ}\text{C}$. We infer that the LL chondrite parent body broke up at near-peak temperatures, quenching in the high T_{REE} and T_{BKN} . Slower cooling at lower temperatures suggests the LL chondrites reaccreted to form a rubble pile parent body while ^{26}Al (or another heat source) was still active.

References: [1] McSween H.Y. et al. (2002) *Asteroids III*, U. Arizona Press, 559–571. [2] Liang Y., Sun C., Yao, L. (2013) *GCA*, 102, 246–260. [3] Dygert N., Liang, Y. (2015) *EPSL*, 420, 151–161. [4] Wang, C., Liang, Y., Xu, W. (2015) *Lithos*, 224–225, 101–113. [5] Liang, Y. et al. (2012) *LPS XLIII*, Abstract #1987. [6] McSween H.Y., Patchen, A. D. (1989) *Meteoritics*, 24, 219–226. [7] Alexander C.M. O'D. (1994) *GCA*, 58, 3451–3467. *XXVII*, 1344–1345. [8] Brey, G.P., Köhler, T. (1990) *J. Pet.*, 31(6), 1353–1378. [9] Marshall, E., et al. (2017) *Geology* 45(6), 519–522. [10] Cherniak, D.Y., Liang, Y. (2007) *GCA*, 71, 1324–1340. [11] Dygert, N., Kelemen, P., Liang, Y. (2017) *EPSL*, 465, 134–144. [12] Taylor, G.J., et al. (1987) *Icarus*, 69, 1–13. [13] Göpel, C., Manhès, G., Allègre, C.J. (1994), *EPSL*, 121, 153–171. [14] Pellas, P., Storzer, D. (1981) *PRSL*, 374, 253–270. [15] Pellas, P., Fieni, C., (1988) *LPS IXX*, 915–916.